

CHAPTER-IV

C H A P T E R - I V

STRUCTURAL, ELECTRICAL, AND OPTICAL PROPERTIES OF

 Bi_2S_3 THIN FILMS.

4.1 Introduction.	106
4.2 Experimental.	108
4.3 Results and Discussion.	108
4.3.1 Finalisation of deposition conditions.	109
a) Deposition temperature.	
b) Deposition time.	
c) Geometry of the substrate holder.	
d) Substrate rotation speed.	
4.3.2 Structural properties.	113
a) Microscopic observations.	
b) XRD studies.	
4.3.3 Electrical properties.	114
a) Conductivity.	
b) Thermoelectric power (TEP).	118
4.3.4 Optical properties.	

4.1 Introduction:

The minimum requirements of a photoelectrochemical cell, consisting of three components viz, a photoelectrode, an electrolyte and a counter electrode are summarised in chapter -I. The basics involved in thin film deposition processes, nature of the semiconductor/electrolyte interface and charge transfer reactions in dark and under illumination have been briefly outlined in chapter II. The experimental processes involved and fabrication and design aspects are high lighted in chapter III.

In this chapter attempts have been made to focus the light on the experimentations involved in a few of the phases of the work such as microscopic observations, XRD studies, conductivity and thermoelectric properties and optical absorption studies. Both theoretical and experimental observations have been examined and compared.

Although, semiconductor/electrolyte junction is simple and easy to device, its properties are sensitive function of the properties of a photoelectrode, an electrolyte and the counte electrode. The effective performance of a PEC cell is found to rely mostly on the photoelectrode properties. Thus performance of a PEC cell is found to depend mostly on the photoelectrode properties. Thus prehistory of the photoelectrode material is a need to know. Any change in the photoelectrode material properties such as

electrical conductivity, thermoelectric power, optical absorbance, bandgap etc., alters both the electrical and optical properties of a PEC cell. Especially, the charge transfer rate across the interface, generation of the short circuit current (I_{sc}) and open circuit voltage (V_{oc}) in a cell are closely related to the properties of semiconductor electrode, an electrolyte and the nature of the junction between them. Thus the detailed characterisation of a photoelectrode material is highly advisable.

Since bismuth trisulphide films are prepared by a chemical deposition process, the preparative deposition conditions and parameters like deposition temperature, speed of the rotation of the substrates, molar concentration of the reactants, deposition time, substrate holder geometry etc. affect the growth mechanism reflecting into the quality and physical appearance of the samples. All these preliminaries are stabilised in the first few stages of the work and are discussed in brief in section 4.3.1. Generally the films, by this technique, are highly resistive than the films deposited by other techniques.

Section 4.3.2 gives information about the microscopic and XRD observations. The electrical and optical studies (conductivity, TEP, optical absorbance, band gap etc.) on thin films is presented in 4.3.3 and 4.3.4 respectively.

4.2 Experimental :

Thin films of bismuth trisulphide were deposited onto amorphous glass substrates as per the procedure outlined in the section 3.3. The crystal structure of the samples was studied with an optical microscope and the XRD techniques. The microstructure was observed with a photospectrometer, Leitz Laborlux, 12 POL. The XRD pattern of both thin film and powdered samples were recorded within the span of angles between 10° to 80° by an X-ray diffractometer with $\text{CuK}\alpha$ lines. The operating conditions of the diffractometer were 30 mA and 20 kV. The dc electrical conductivity (σ) and thermoelectric power (p) in dark were measured for the samples as explained in section 3.4.3 and 3.4.4 respectively. The ranges of working temperature were 300 K to 600 K and 300K to 500 K respectively and the temperature was controlled to 1°C . The optical absorption measurements were performed as mentioned in section 3.4.5. The working range of wavelength was from 4000 \AA to 9000 \AA .

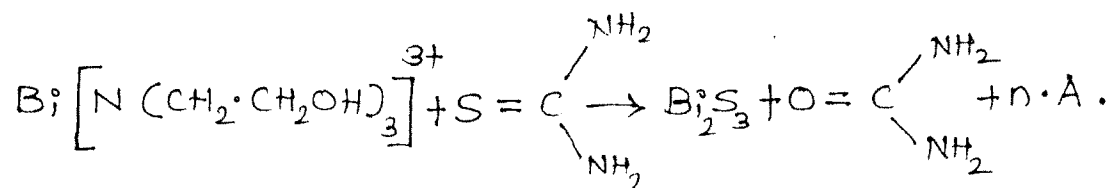
4.3 Results and Discussion :

Preparation of thin film photoactive materials play an important role in devising photoelectrochemical solar cells. Thin film photoactive electrodes have the over riding advantages of ease of preparation and cheapness because of the very small quantity of the active materials required. A quality thin film material results, if number of preparative

parameters such as, deposition temperature, deposition time, speed of substrate rotation, pH and concentration of basic ingredients etc. are optimised. Following are few of the possible parameters studied in brief while depositing the samples.

4.3.1 Finalisation of deposition conditions :

The thin films of Bi_2S_3 are prepared by a solution growth technique. The mechanism and process of film formation from triethanolamine complex of Bi^{3+} and thiourea with a little NH_4OH is discussed in section 2.3. Triethanolamine forms a complex compound with bismuth nitrate. The dissociation of thiourea occurs in an alkaline medium when the temperature of reaction container is raised to 95°C to form a Bi_2S_3 nucleus. The reaction mechanism can be expressed as :



where, A is complexing agent $\text{N}(\text{CH}_2\text{CH}_2\text{OH})_3$. The process of formation of bismuth trisulphide films is found to be a strong function of various preparative parameters and deposition conditions. The various factors over viewed are :

a) Deposition temperature :

As thiourea dissociates at a certain temperature, the deposition temperature plays an important role while

preparing the Bi_2S_3 samples. In a reaction vessel there is no any means to speed up the decomposition of thiourea. As a result film formation is expected to take place above a certain temperature wherein thermal energy helps to decompose thiourea and provides kinetic energy to the ions resulting into an increased number of collisions and hence the film formation occurs. The films were deposited at various temperatures from 80°C to 130°C with an interval of 10°C . Below 90°C the films are difficult to obtain. At high temperatures the films are formed, however, are relatively nonsticky and nonuniform. At moderate temperatures (95°C to 110°C), the physical appearance of the samples (uniformity, stickiness, thickness etc.) showed that the films deposited at $95 \pm 2^\circ\text{C}$ are more suitable than others.

b) Deposition time :

As thiourea dissociates slowly the deposition of Bi_2S_3 films is a slow process. Further, it is found that the deposition at 95°C results in uniform, highly adherent, specularly reflecting thin films [42 43] and a saturation in film thickness is observed after 35 minutes. A deposition time of approximately 40 minutes was selected to ensure maximum thickness [42,43].

c) Geometry of the substrate holder

A substrate holder designed in our laboratory (section 3.2.4) was used to fix the position of the rotating

samples. It was found that the substrates at 90° each other gave uniform deposits implying that the geometry of the substrate holder allows required crystal orientation [43]. A substrate holder in which substrates makes an angle of 90° with the respective diameter is used in further study.

d) Substrate rotation speed.

The speed of the rotation of the substrates is the key factor in deciding the thickness of the deposit. An uniform speed of substrate rotation was varied with the help of constant speed ac gear motor from 50 r.p.m. to 150 r.p.m. It was found that the deposit thickness goes on decreasing as the speed increases as shown in fig.4.1. For any speed in low speed range (50 to 65 r.p.m.) films are found to be thick, non specular and spotty. Further, they are less adherent in this range. In the medium range of speeds (65 to 90 r.p.m.) moderately thick, diffused reflecting and highly adherent deposits are obtained. At higher speed of rotation the films are thin, specularly reflecting and adhesive. Attempts were made further to deposit Bi_2S_3 layers on stationary substrates indicating the powdery, porous, thick, less uniform and non reflecting deposits. The effect of speed would seem to imply that the fluid motion prevents adhesion of the precipitated Bi_2S_3 to the surface of the substrates. In this study an intermediate speed of about 70 r.p.m. was chosen and kept constant.

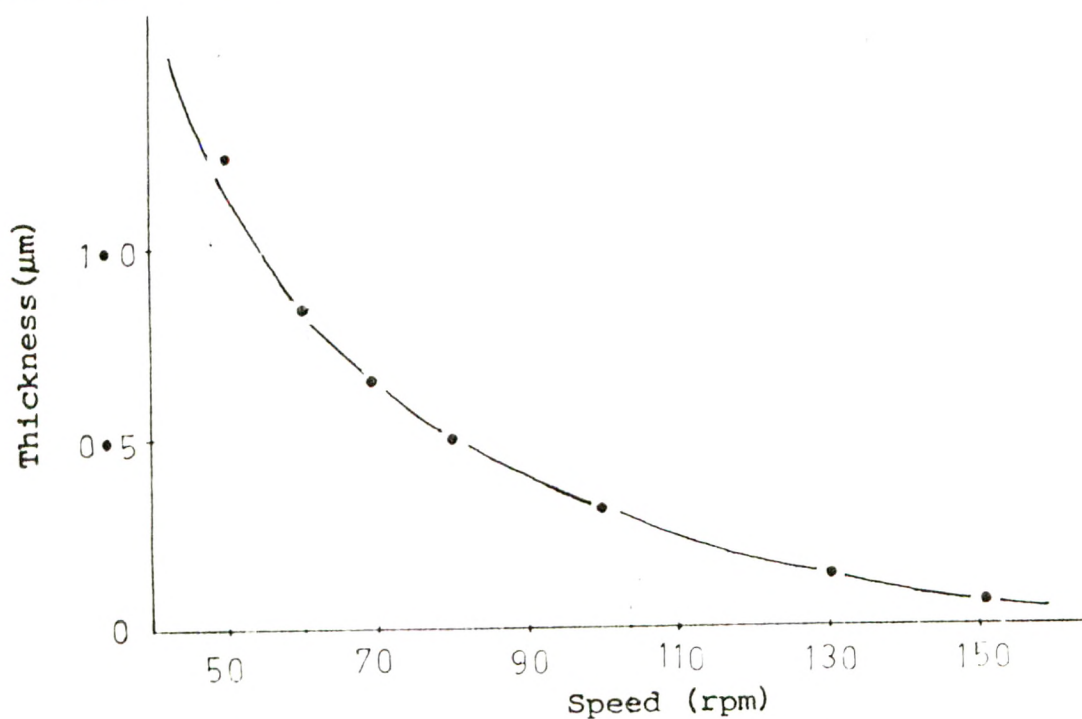


Fig.4.1. Dependence of film thickness on speed of substrate rotation.

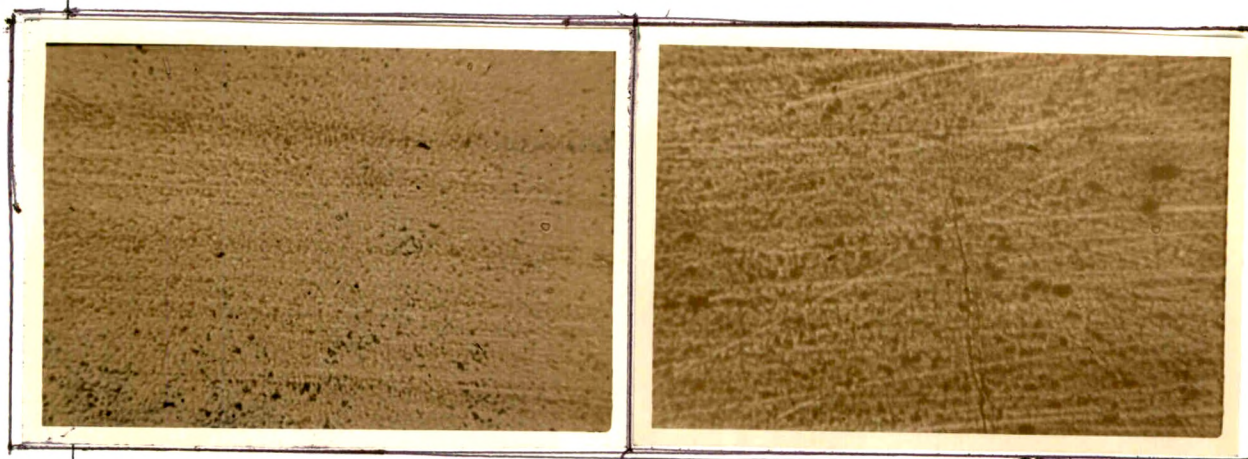


Fig.4.2. Crystal structure of Bi_2S_3 ;

- 1) as deposited, and
- 2) heated at 200°C.



4.3.2 Structural properties :

Studies on structural aspects of bismuth, antimony and arsenic sulphides have been chiefly restricted to physically vapor deposited films. However, homogeneous films have been also obtained by some other techniques [44,91-95]. The literature survey reveals that the conventional solution growth methods are being widely used for the growth of binary and ternary compounds owing to their easiness and simplicity. Not much data is available on the subject.

a) Microscopic observations :

The crystal structure of a thin layer of Bi_2S_3 is shown in fig. 4.2. The films are found to be polycrystalline with defined grain boundaries and homogeneous in nature. The crystallinity improves after heating the samples for temperatures higher than the deposition temperature.

b) XRD studies :

The structure and crystallinity was also tested by XRD patterns in the span of angles between 10° to 80° . The XRD of thin films and powder was obtained. The d' values of the lines are obtained directly from a computerised data and are compared with standard d' values from A.S.T.M. data for Bi_2S_3 . The observed d' values are in excellent agreement with the standard d' values of the material. This confirms that the material is purely Bi_2S_3 . The comparison of d' values is shown in table 4.1. The XRD data clearly indicates that

the films are polycrystalline and peak intensities corresponding to different crystallographic planes are higher. These are also listed in table 4.1. The peak intensities and 'hkl' values obtained for Bi_2S_3 shows the orthorhombic structure of the material [96].

4.3.3. Electrical properties :

As is mentioned earlier, the bismuth trisulphide is a member of V and VI compound semiconductors and is of technologically important in view of its higher photosensitivity, photoconductivity and thermoelectric power [16-18,26,44,92,97-101]. The literaturistic data accounts very rare references on the subject, however, some reports are available on both amorphous as well as crystalline materials [16-18,26,44,92,97-101]. This section presents some of the observations on d.c. electrical conductivity and thermoelectric power.

a) Conductivity :

The samples were tested for their electrical conductivity in the temperature range 300 K to 600 K (as stated in chapter - III for both heating and cooling cycles. The change in conductivity is noted for every 5°C rise in temperature. The conductivity is found increased with increasing temperature indicating the semiconducting nature of the samples prepared by our chemical deposition process [42,43]. The temperature dependence of conductivity is shown

in fig.4.3. It is understood that both for heating and cooling cycles, $\log.6$ vs $1/T$ variation follows almost the same track over the temperature range studied. This also confirms the uniformity of the samples. Further, the plot shows clearly two distinct regions corresponding to two values of activation energies. In high temperature region the variation of $\log.6$ is rapid as compared with low temperature region. This can be ascribed to the fact that, at high temperature region, the thermal energy is sufficiently high to create vacancies and activation energy for the creation of vacancy, which is responsible for the motion of charge carriers within the vacancies. On the other hand, at lower temperature, the thermal energy is only large enough to allow the migration of charge carriers into vacancies already present in the material contributing to the approximately constant variation of $\log.6$ with temperature as shown in fig. 4.3 [102].

In general, resistance of bismuth sulphide thin films is very high compared to the single crystal resistance and this is mainly because of the grain boundary discontinuities and thickness of the films. Moreover the grain boundary and discontinuity of the samples are dependent on the deposition conditions [16,42].

The thermally activated conductivity and activation energy in the low and high temperature regions are related

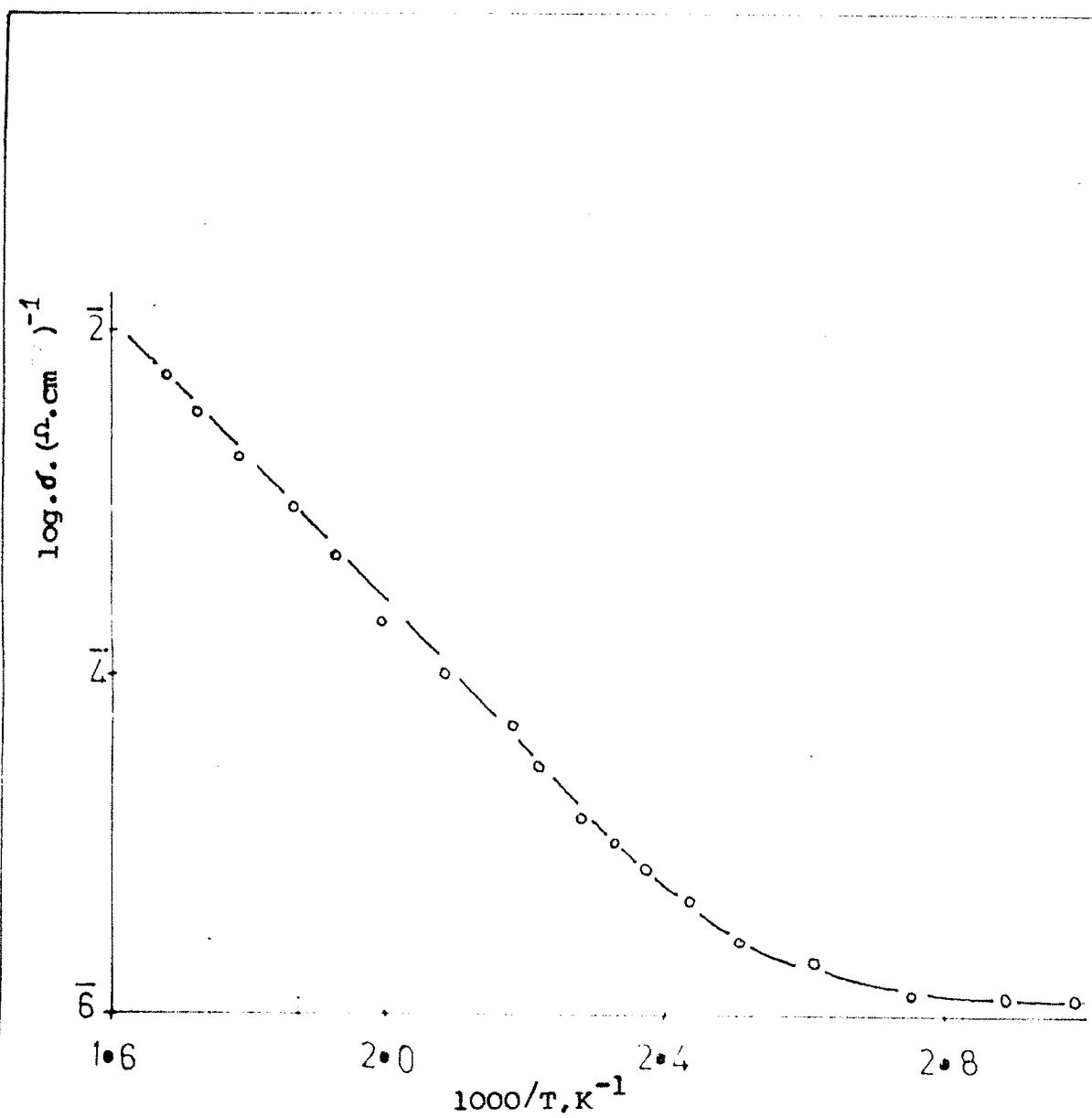


Fig.4.3. Temperature dependence of conductivity for Bi_2S_3 thin films

as:

$$\sigma = \sigma_0 \exp(-E_a/kT) \quad \dots 4.1.$$

where, σ = conductivity of the sample,

E_a = activation energy in eV,

K = Boltzmann's constant and

T = absolute temperature.

The activation energies of electrical conduction have been determined in low and high temperature regions and found to be 0.16 eV and 0.80 eV respectively. A considerable difference is observed in the values of activation energies in our case and the values so far reported [16, 44, 103]. This can partly be attributed to comparatively lower resistivity of our samples than the samples prepared by other techniques such as : Solution gas interface technique, dip and dry, sulfurisation and spray pyrolysis. The lower resistivity can also be due to the relatively higher thickness, improved degree of crystallinity provided by the preferred orientation while depositing the samples. We believe that this flexibility can thus be accounted for the use of substrate holder design [39,42]. This is also reflected in the lower magnitudes of activation energies. [16,42].

b) Thermoelectric power (TEP):

Another technique to characterise the thin films electrically is the measurement of thermoelectric power (TEP) as a function of temperature. The technique helps to detect

the type of material under investigation. Thermoelectric power (p) measurements were carried out in the temperature range 300 K to 500 K, and the polarity of the thermally generated voltage is negative towards the hot end of the samples. The temperature variation of thermoelectric power is depicted in fig.4.4. It is found that the samples are of n-type conduction. The thermoelectric power, p , varies according to the relation [18,19]:

$$p = -\frac{k}{q} \left[A + \ln \cdot \frac{2(2m_e^* \cdot kT)^{\frac{3}{2}}}{nh^3} \right] \quad \dots 4.2.$$

where, q = electronic charge,

h = Planck's constant, A = thermoelectric factor introduced by the kinetic energy of electrons and hence depends on the scattering process, n = carrier concentration, m_e^* is the effective mass of an electron, k = Boltzmann's constant and T = absolute temperature. P for Bi_2S_3 material in thin film form is of the order of microvolts. Thermoelectric power is observed to increase with increase in temperature. The results are in close agreement with that of the others.

4.3.4 Optical properties:

The material is further characterised by means of an optical method to know the type of the transition, the optical absorbance and the optical band gap. The absorption spectra has been studied at 300 K in the wavelength range from 400 nm to 900 nm. The absorption coefficient is of the

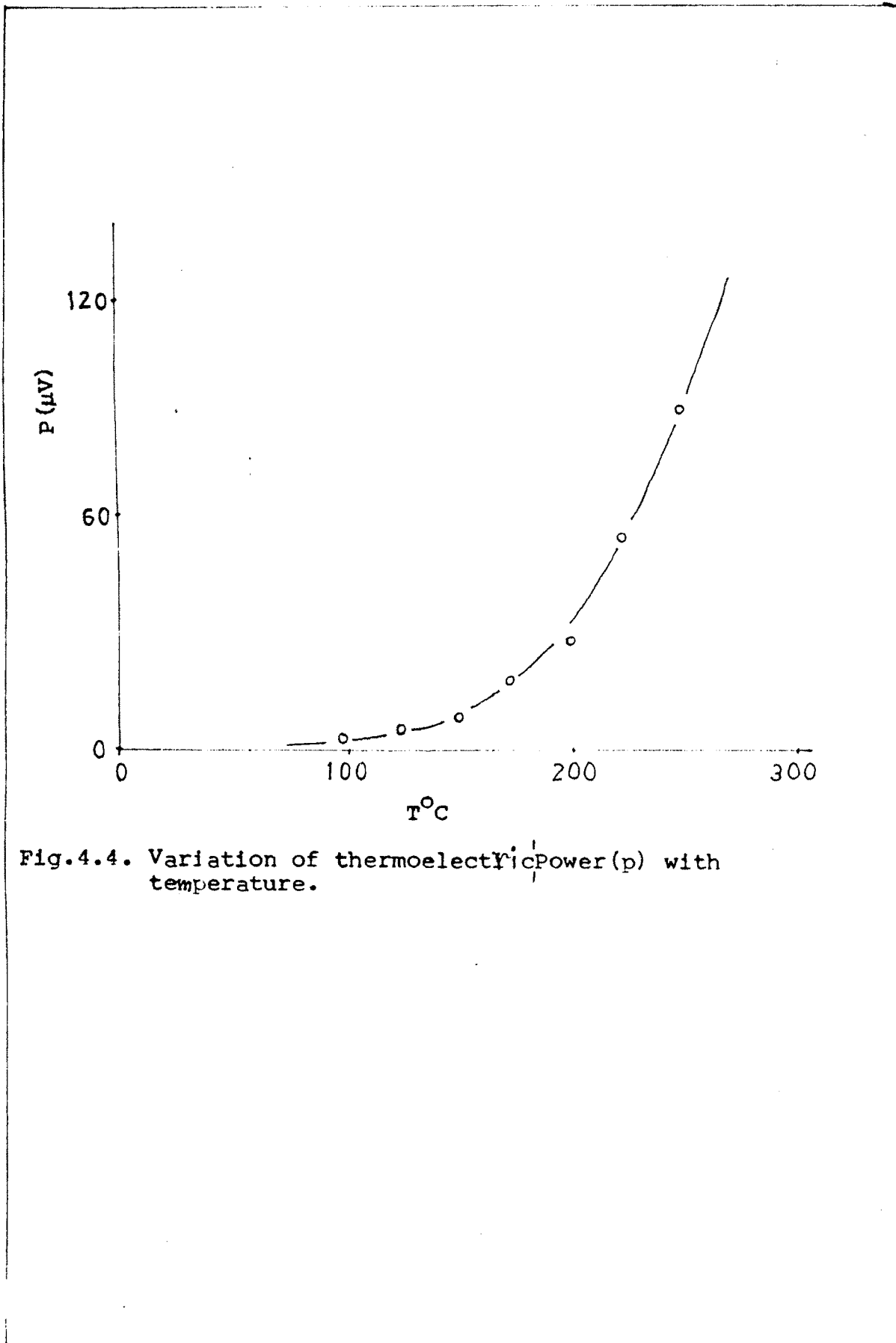


Fig.4.4. Variation of thermoelectric power (p) with temperature.

order of 10^4 cm^{-1} , indicating that the material is of the direct band gap type and the transitions are allowed [16,44,103]. The energy absorbance spectrum is shown in fig.4.5. Following the usual theoretical analysis the energy dependent absorption coefficient can be expressed by the relation for both allowed direct and indirect transitions as [105]:

$$\alpha_{d,i} = B \cdot (h\nu - E_{d,i})^n \quad \dots 4.3.$$

where, B is a constant, E_d and E_i refer to the direct or indirect band edges. For direct transitions n assumes a value of 1/2 and 2 for indirect transitions. For large α (10^4 to 10^5 cm^{-1}), corresponding to the photon energies near the band edges a direct transition has been reported for Bi_2S_3 [106, 107]. Thus, α for allowed transition can be determined using equation 4.3. These observations are in good agreement with the fact that the material under study is essentially known to be direct gap with $n = 1/2$ [15]. The absorption edge is much broader than that expected for a direct gap materials. This broadening of an absorption edge results in a deviation from linearity in the low energy side. This can be ascribed to the grain boundary effect in the structure and little amount of lack of stoichiometry generally observed in polycrystalline materials [42,103,106].

For Bi_2S_3 thin films, the absorption is explained on the basis of exciton formation [103], however, our

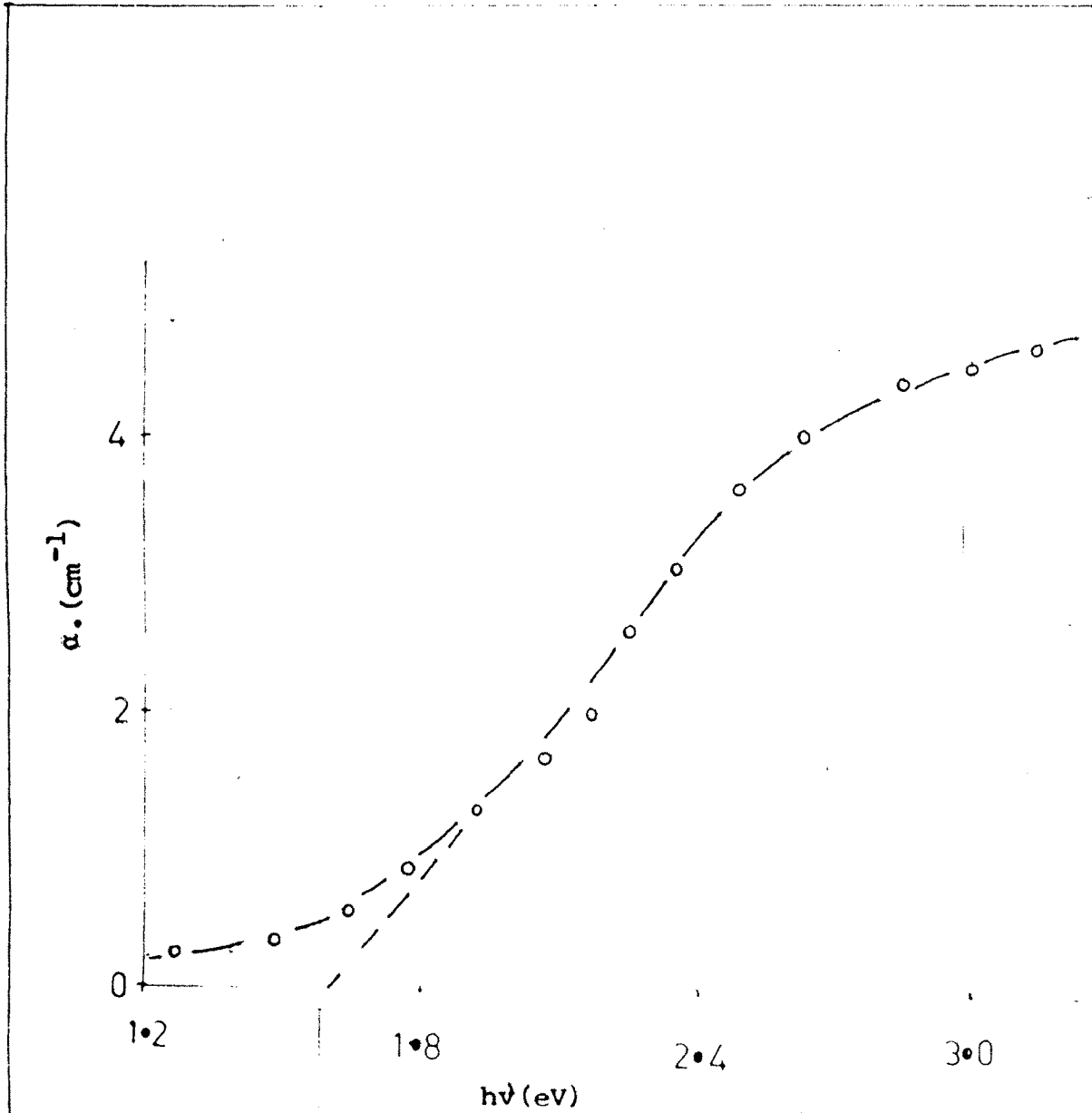


Fig.4.5. Energy absorption spectrum for chemically deposited Bi_2S_3 thin films.

measurements are at room temperature and it is expected that at this temperature the exciton band is absent. Thus absorption will be due to only a band to band transition. This can be explained by plotting $(\alpha h\nu)^2$ vs $h\nu$ as shown in the fig.4.6. The extrapolation of the plot to the energy axis gives a value of band gap equal to 1.60 eV. This agrees well with the values reported by others. The magnitude seems to be higher than that for a single crystal Bi_2S_3 [42,103,107]. The difference can be accounted for interference by diffused reflectance within the material itself [26] and may be due to the anisotropy of the film formation process [16,42,43]. Bhattacharya and Pramanik [16] reported the bandgap of chemically deposited Bi_2S_3 to be 1.47 eV.

In accordance with their observations, the higher bandgap of chemically grown Bi_2S_3 thin films is due to the mixture of amorphous and crystalline phases. We got the similar observations hence we have heat treated the samples just above the deposition temperature.

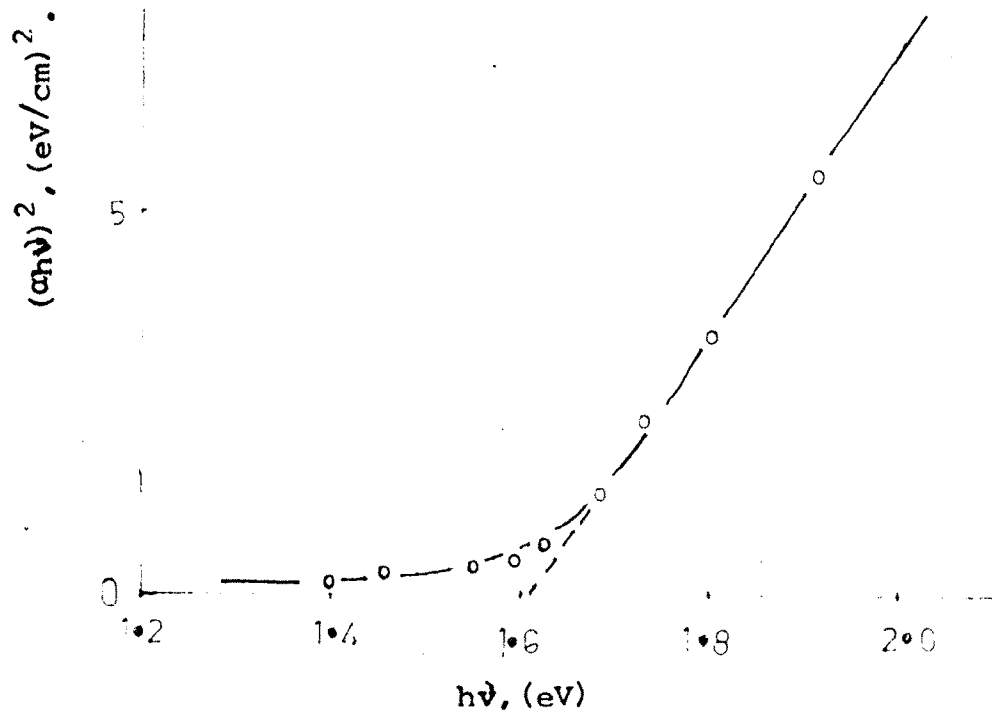


Fig.4.6. Determination of optical bandgap from variation of $(\alpha h\nu)^2$ vs. $h\nu$.

Table 4.1 : d values of Bi_2S_3 film powder calculated from powder diffraction pattern.

Sr.No.	Angle 2θ	d-observed \AA	d-ASTM	I/ I_{max}	hkl
1	25.46	3.51	3.56	42.98	130
2	28.54	3.12	3.12	39.3	230
3	33.49	2.67	2.71	47.46	301
4	33.685	2.66	2.64	67.60	221
5	40.8	2.21	2.26	42.98	141
6	41.44	2.177		47.46	
7	41.85	2.1567		44.44	
8	43.95	2.06	2.01	100.00	
9	44.12	2.05		58.78	431
10	51.18	1.78		42.98	
11	51.48	1.77	1.74	52.16	061
12	60.59	1.53	1.48	40.11	
13	70.1	1.34		75.11	
14	72.92	1.296		44.44	
15	75.47	1.259		69.44	